Universiteit Utrecht

Faculteit Bètawetenschappen

A simulation study of quasicrystaline phases and structural cross-over in binary hard-sphere mixtures.

Bachelor Thesis

Tom de Vries

Natuur- en Sterrenkunde

Supervisor:

Dr. Marjolein Dijkstra
Debeye Institute

June 12, 2019

Abstract

Using NVT Monte Carlo simulations an attempt is made to discover a quasicrystaline phase in a binary mixture of hard spheres. This is done by finding and following the structural cross-over line calculated theoretically by Statt et al. [Sta+04]. This line separates the (η_s, η_b)-plane into two areas where the pair correlation function has a wavelength on the order of the big and small particles' size respectively. At this cross-over line there should be competing length scales in the system, which is common in quasicrystals. The pair correlation function is measured from simulations at different total- and relative packing fractions. The wavelength is measured for all of them, and an area in the (η_s, η_b)-plane where structural crossover occurs is extrapolated. Although no quasicrystals were found in any of the simulations, the data collected on the structural cross over could prove valuable in doing so in the future.

Contents

1 Introduction

In this work we will make an attempt at figuring out what conditions will allow the formation of a quasicrystaline phase in a binary hard sphere mixture. We will use a Monte carlo simulation to simulate a set of particles with two different sizes. The diameter of the larger particles is used as the unit of length, the diameter of the smaller particles is therefore the same as the ratio between the two diameters λ. By varying the packing fractions of the particles, we attempt to find an initial setup that causes the particles to form a quasicrystal. First, we will look into what a quasicrystal actually is in this section. In section 2 we will discuss the methods by which we will simulate the system. Then we will discuss the results of our simulations in section 3. And finally, we will make some concluding remarks in section 4

Quasicrystals are solids that exhibit many crystal-like properties, but do not adhere to some of the 'rules' for crystals. In a regular crystal, particles are aranged in a lattice. This means that in a k-dimensional system, one can define a set of k lattice vectors such that a vector pointing from any partilce to any other particle can be obtained using an integer sum of the lattice vectors. In addition, any vector that is an integer sum of the lattice vectors will point from any particle to another particle. This means that crystals are periodic structures, and have translational symmetry with respect to translations along integer sums of lattice vectors. A crystal can be defined by a single piece of it, a unit cell, that is copied an infinite amount of times, filling all of space.
The requirement that all of space must be filled with only copies of the same unit cell means that unit cells can only posses 2-, 3-, 4-, and 6-fold rotational symmetries (see figure 1), as only shapes with these symmetries can fill all of space alone.

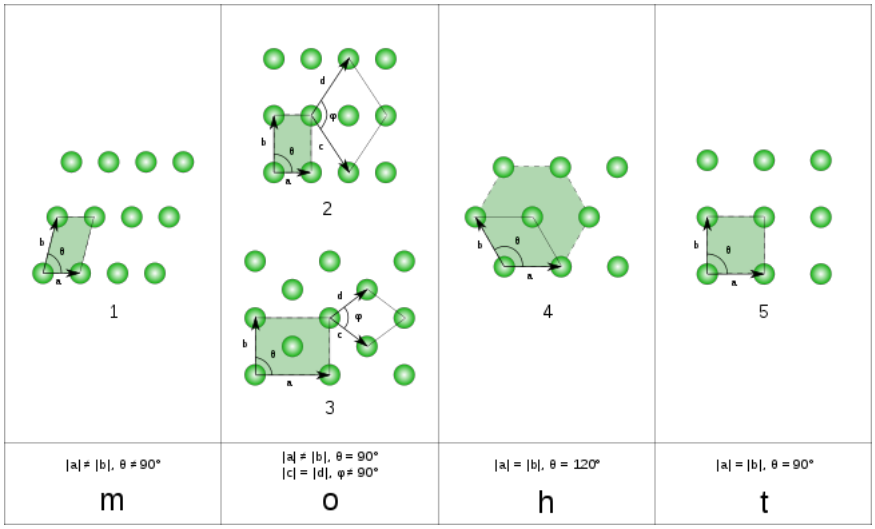

Figure 1: The 2-dimensional Bravais lattices. It should be possible to describe any crystal (in 2D) using one of these lattices. All of them have 2-fold symmetry, number 4 also has 3- and 6-fold symmetry, and number 5 also has 4-fold symmetry. A similar set exists for three dimensional lattices.[Kit96]

Quasicrystals differ from regular crystals in that they have quasi-periodic translational order [LS84]. This means they appear to possess periodic translational order, but they actually do not. Particles in a quasicrystal are not on a regular lattice. This means that one cannot define a single unit cell to describe the whole system.
All of this does not mean that quasicrystals are disordered. Using multiple different shapes, all of space can still be filled (see figure 2). Quasicrystals can posess rotational symmetries not found in regular crystals. For example, the one in figure 2 has 5-fold rotational symmetry.

In mathematics, the idea of differently shaped 'tiles' filling all of space has been around since the nineteen sixties. Roger Penrose and other mathmaticians tried to come up with ways of filling space using tiles with symmetries other than 2, 3, 4, or 6. Penrose found one way of doing so using a set of tiles shown in figure 2. [RPe79]

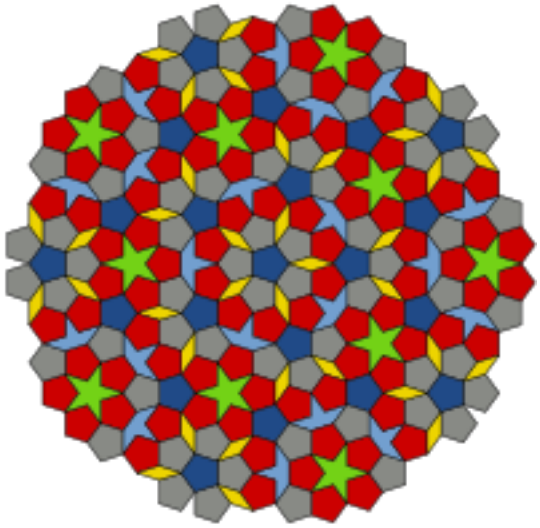

Figure 2: A penrose tiling, these tiles can fill all of space in an aperiodic fashion. This is often used as a visual example of a quasicrystal.[GS16]

The first documentation of what we now call a quasicrystal appeared in november of 1984, when Schechtman et al. reported finding a "metallic solid with long-range orientational order, but with icosahedral point group symmetry, which is inconsistent with lattice translations."[DSh+84]. Soon after, Levin et al. [LS84] described quasicrystals more exactly in their work "Quasicrystals: a new class of ordered Structures" and confirmed that the findings of Schechtman et al. matched their definition.
Quasicrystals can form when there are multiple different relevant length scales in a system. This can happen because there are forces with different behaviors at different ranges, or because the interactions between the particles have multiple distances at which a particle can remain (meta)stable. We will be working with a binary mixture, which means there are two kinds of particles with different sizes. Because there are bigger and smaller particles, there are two relevant length scales: the radius of the big particles and the radius of the smaller particles.

Some applications for quasicrystaline materials have been proposed by Dubois et al. [DKP94]. They conclude that their low friction coefficient and malliability at high temperatures make quasicrystals useful as a coating on softer materials to prevent wear and tear. Quasicrystals also have much lower electrical and thermal conductivity than one would expect from a metallic solid. This means they could also serve as insulation materials.

Quasicrystals have been observed experimentally in binary mixtures before[Tal+09]. But in this work we will use Monte Carlo simulations to investigate quasicrystals in binary mixtures. Finding a quasicrystal using simulations might give us more insight into the theory behind the way quasicrystals form.

To find a quasicrystal we should start by finding a way to get two competing length scales. We already have two length scales: the diameters of the two types of particle. But we need to find a setup in which both are 'competing for dominance' so that multiple different shapes form in the structure of the system.

A good place to start could be the structural cross-over line described by Statt et al.[Sta+04]. In their article they describe the cross-over line as a curve in the space of relative packing fractions. On one side of this curve the diameter of the bigger particles is the most relevant length scale, and on the other side the diameter of the smaller particles is the most relevant length scale. We will go more in depth about the cross-over line in section 2.

2 Method

We will use NVT Monte Carlo simulations to try and create a quasicrystal. In this Section we will first explain what a monte carlo simulation is and how it works. Second, we will introduce our system and its specifics. Third, we will discuss how we intend to find the right initial conditions for the formation of a quasicrystal. And finally, we will show how our similation works and what it does.

2.1 Monte Carlo

Normally, to find values for certain observables in a many-particle system, one would need to average over a large set of configurations in the system. Averaging over all of the configurations would be impossible, as there are an almost endless number. Simply generating a lot of random configurations isn't desirable either, as the Boltzmann distribution tells us not all configurations are equally likely [BB10]. A Monte Carlo simulation makes use of the Boltzmann distribution to generate configurations according to their correct statistical weight. The Monte Carlo simulation begins by taking a starting configuration, either randomly generated or pre-created, and calculating its Boltzmann weight.[BB10]

$$W_{Boltz} = e^{-\beta E}, \quad \beta = \frac{1}{k_b T} \tag{1}$$

This weight depends on the potential of the system, and thus on the interaction potential between particles. We will discuss the interaction potential of our system below. After calculating the weight, the simulation tries to make a change by moving a particle, adding a particle, changing the volume, or something like that. Ours is an NVT Monte Carlo simulation, which means the number of particles(N), the volume(V) and the temperature(T) are fixed. This means the only change left is moving a particle. Then the simulation calculates the Boltzmann weight after the attempted change. If the weight after the change is larger than the weight before the change, the move is always accepted. If the weight after the change is smaller than the weight before the change, the move has a chance of $\frac{W_{before}}{W_{after}}$ to be accepted. This means the chance of being accepted is

$$P_{acceptance} = \begin{cases} 1 & W_{before} \leq W_{after} \\ \frac{W_{before}}{W_{after}} & W_{before} > W_{after} \end{cases} \tag{2}$$

Before measurements can start, the simulation needs to equilibrate. This is because the starting configuration might not be a configuration with a very high probability. The system must be allowed to equilibrate for quite a while to ensure fluctuations in observables due to the starting configurations are not taken into the measurements. The process of reaching equilibrium can take thousands of Monte Carlo cycles to complete, a monte carlo cycle is an amount of attempted moves roughly equal to the amount of particles in the system. After the system has reached equilibrium, the relevant observable is measured at regular intervals. The measured observable can then be averaged over all the measurements. Because the simulation already generates configurations with their correct statistical weight, there is no need to take these weights into account further when averaging (provided the system was given enough time to equilibrate and enough measurements were taken).

2.2 System specifications

To use a Monte Carlo simulation, we need a system to work on. In this work we will be making use of a binary hard sphere mixture, we'll discuss what that means now. The term 'binary mixture' refers to the fact that in our system, there are two different kinds of particles mixed together. We refer to these particles as Big (b) and Small (s), any variable (A) specifically associated with either the big particles or the small particles will be written as A_b or A_s respectively. The particles have a size ratio $\frac{\sigma_s}{\sigma_b} = \lambda$, where σ_b and σ_s are the diameters of the two particle types

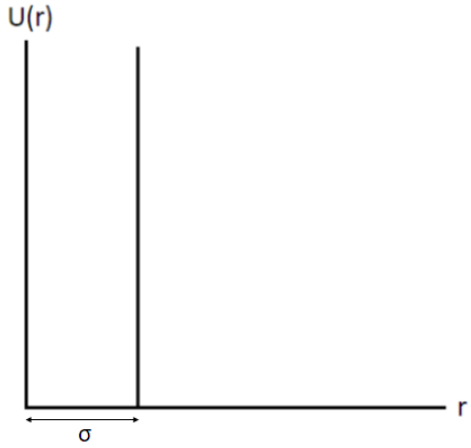

Figure 3: The hard core potential, r is the distance between the centers of two particles and $U(r)$ is the potential between the two. [PJ17]

The 'hard sphere' part of the system refers to the way the particles interact with one another. The interaction potential we use here is the hard core potential, this is one of the very simplest interaction potentials you can think of (aside from perhaps the ideal gas, where the potential is always zero). The hard core potential is a function of the distance between the centers of particles, it is zero everywhere exept the region in distance space where the particles would overlap, the potential in that region is taken to be infinite. Because we have two types of particles, we need three different potentials, ϕ_{bb}, ϕ_{ss}, and ϕ_{bs}, these are given by:

$$\phi_{bb}(r) = \begin{cases} 0 & r > \sigma_b \\ \infty & r \leq \sigma_b \end{cases}, \quad \phi_{ss}(r) = \begin{cases} 0 & r > \sigma_s \\ \infty & r \leq \sigma_s \end{cases}, \quad \phi_{bs}(r) = \begin{cases} 0 & r > \frac{\sigma_b}{2} + \frac{\sigma_s}{2} \\ \infty & r \leq \frac{\sigma_b}{2} + \frac{\sigma_s}{2} \end{cases}, \tag{3}$$

From now on, we will take the diameter of the big particles to be our unit of length. The small particles will therefore have a diameter of λ. The total energy of the system is easily calculated using this potential, as even a single overlap will immediately turn it infinitely large. The total energy is thus 0 if there are no overlaps, and infinite if there are any. This means we can calculate the probability of a move being accepted using equations 1 and 2. If we use that $lim_{x\to\infty} e^{-\beta x} = 0$ we find:

$$P_{acceptance} = \begin{cases} 1 & no\ overlaps \\ 0 & otherwise \end{cases} \tag{4}$$

As you can see, as long as no two particles occupy the same space, any move is accepted.

As mentioned earlier, to get the simulation going you need a starting configuration. In the simulations we used two different starting configurations with different advantages. These are described in two dimensions, as this is what we mainly used, but everything translates fairly easily to three dimensions.
The first starting configuration we used is a centered square crystal phase. In this configurations the particles are placed in a regular lattice. The big particles are placed in a square shape with regular distances between them, then a small particle is placed in the center of each square. The advantage of this is that it takes very little time for the simulation to set up. A disadvantage is that the number of particles cannot be set freely, and the numbers of small and big particles have to be always equal
The other starting configuration is a fluid phase, in which all the particles are simply given random postitions until none of them overlap. The advantage here is that the number of small and big particles can both be set to whatever value you want. A disadvantage is that the simulation takes a very long time to set up this configurations at higher packing fractions.

2.3 How to find a quasicrystal

To find a quasicrystal we could just scan all of (η_b, η_s)-phase space for several values of λ and hope to find one. But that would take much too long. Instead we will use some previous research to get an idea of the area in phase space we need to look at. The methods we used to find the right state point are similar to those used by Statt et al.[Sta+04] and Evans et al.[REv+94]. We try to find the line in (η_b, η_s)-space where the wavelength of oscillations in the pair correlation function ($h(r) = g(r) - 1$) changes abruptly from roughly the diameter of the big particles to roughly the diameter of the small particles. The wavelength of oscillations in $h(r)$ is given by $\frac{2\pi}{\alpha_1}$ with α_1 the real part of the leading pole of $h(r)$. These poles come from the Fourier-space Ornstein-Zernike equations for binary mixtures[FG57]:

$$\hat{h}_{ii}(q) = \frac{\hat{c}_{ii}(q) + \rho_j[\hat{c}_{ij}^2(q) - \hat{c}_{ii}(q)\hat{c}_{jj}(q)]}{D(q)} \tag{5}$$

$$\hat{h}_{ij\neq i}(q) = \frac{\hat{c}_{ij}(q)}{D(q)} \tag{6}$$

$$D(q) = [1 - \rho_b\hat{c}_{bb}(q)][1 - \rho_s\hat{c}_{ss}(q)] - \rho_b\rho_s\hat{c}_{bs}(q) \tag{7}$$

Here $\hat{h}(q)$ and $\hat{c}(q)$ are the Fourier transforms of $h(r)$ and $c(r)$ respectively, and i,j can refer to the big(b) and small(s) particles. The poles are given by $\alpha = \alpha_1 + i\alpha_0$ such that $D(\alpha) = 0$. Since $D(q)$ is the same for all the different $h(r)$s, they all share the same wavelength.
To find the leading pole of $h(r)$, we first measure the three $g(r)$s in the simulation and calculate $h_{ij}(r) = g_{ij}(r) - 1$. We then invert the mixture OZ equations ((5)-(7)) to calculate the three $\hat{c}(q)$s.

$$\hat{c}_{ii}(q) = \frac{\hat{h}_{ii}(q) - \rho_j[\hat{h}_{ij}^2(q) - \hat{h}_{ii}(q)\hat{h}_{jj}(q)]}{E(q)} \tag{8}$$

$$\hat{c}_{ij\neq i}(q) = \frac{\hat{h}_{ij}(q)}{E(q)} \tag{9}$$

$$E(q) = [1 - \rho_b\hat{h}_{bb}(q)][1 - \rho_s\hat{h}_{ss}(q)] - \rho_b\rho_s\hat{h}_{bs}(q) \tag{10}$$

We then use reverse Fourier transformations to find the $c(r)$s.
We obtain a set of equations to solve by entering $\hat{c}_{ij}(q) = 2\pi\int_0^\infty[rc_{ij}(r)J_0(qr)dr]$ into $D(\alpha) = 0$. Here, $J_0(qr) = \frac{1}{\pi}\int_0^\pi[cos(-qrsin(\tau))d\tau]$ is the zeroth order Bessel Function. We can now find a set of equations to solve for α_1 and α_0 by equating the real and imaginary parts. To do that we need to find the real and imaginary parts of $J_0(\alpha_1 + i\alpha_0)$.

$$J_0(qr) = \frac{1}{\pi}\int_0^\pi[cos((-\alpha_1 r - i\alpha_0 r)sin(\tau))d\tau] \tag{11}$$

$$J_0(qr) = \frac{1}{2\pi}\int_0^\pi[e^{\alpha_0 rsin(\tau)}e^{i\alpha_1 rsin(\tau)} + e^{-\alpha_0 rsin(\tau)}e^{-i\alpha_1 rsin(\tau)}d\tau] \tag{12}$$

$$J_0(qr) = \frac{1}{\pi}\int_0^\pi[cosh(\alpha_0 rsin(\tau))cos(\alpha_0 rsin(\tau)) + i\ sinh(\alpha_0 rsin(\tau))sin(\alpha_0 rsin(\tau))d\tau] \tag{13}$$

Now we can separate $D(\alpha_0 + i\alpha_1) = 0$ into real and imaginary parts.

$$1 = \rho_b R_{bb} + \rho_s R_{ss} + \rho_b\rho_s R_{bs}^2 - \rho_b\rho_s R_{bb}R_{ss} \tag{14}$$

$$1 = \rho_b I_{bb} + \rho_s I_{ss} + \rho_b\rho_s I_{bs}^2 - \rho_b\rho_s I_{bb}I_{ss} \tag{15}$$

$$R_{ij} = 2\pi\int_0^\infty[rc_{ij}(r)\frac{1}{\pi}\int_0^\pi[cosh(\alpha_0 rsin(\tau))cos(\alpha_1 rsin(\tau))d\tau]dr] \tag{16}$$

$$I_{ij} = 2\pi \int_0^\infty [rc_{ij}(r)\frac{1}{\pi}\int_0^\pi [sinh(\alpha_0 r sin(\tau))sin(\alpha_1 r sin(\tau))d\tau]dr] \tag{17}$$

This set of equations can be solved numerically to find the wavelength we want.
Now we can find a crossover line like the one described in figure 1 of the article by Statt et al.[Sta+04]. If the packing fraction is increased along this line into the crystal phase, we would have two competing length scales in a solid structure. That might cause a quasicrystaline phase to form. Statt et al. calculated the line theoretically using the Percus Yevick closure. (figure 4)

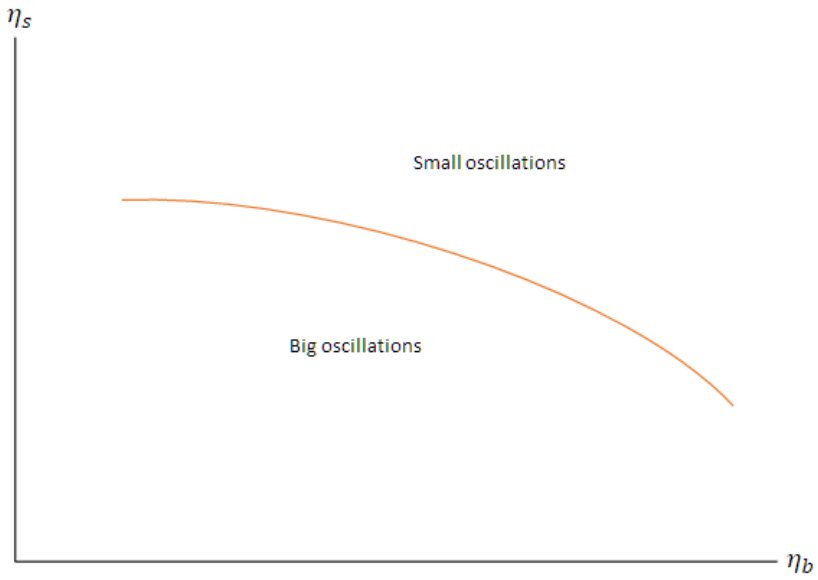

Figure 4: A sketch of the cross over line calculated by Statt et al. [Sta+04] using the Percus Yevick closure.

2.4 Our simulation

Now that all of the basics have been explained, we are going to go through our own simulation step by step, explaing what it does and how it works. Once again, this explaination will assume a two-dimensional system, but it is easily expanded to three dimensions.
Before the simulation can run, it needs a few values to be set, these can be varied between runs so different state points can be considered. The values that can be varied are: the size of the system (L), the total and relative packing fractions (η, η_b, η_s), the size ratio, the number of moves the simulation will attempt, the maximal displacement for a single move (Δ), and the number of measurement points for the calculation of g(r) (more on this later). The amount of moves between two measurements of g(r) and the point at which measurements start can also be set.

The simulation starts by generating a starting configuration. If the starting configuration is a crystal phase, the number of particles, and the distance between them (len) are calculated to match the specified packing fraction as closely as possible while creating an integer number of unit cells. The actual packing fraction this results in is usually close to the set value, but it is rarely exact. This also means the number of particles cannot be set directly. Then a big particle is placed at every point (n*len, m*len) with n and m integers. Every time a big particle is placed, a small particle is placed at position (len/2, len/2) from the big particle. This way they form a centered square crystal (figure 5)

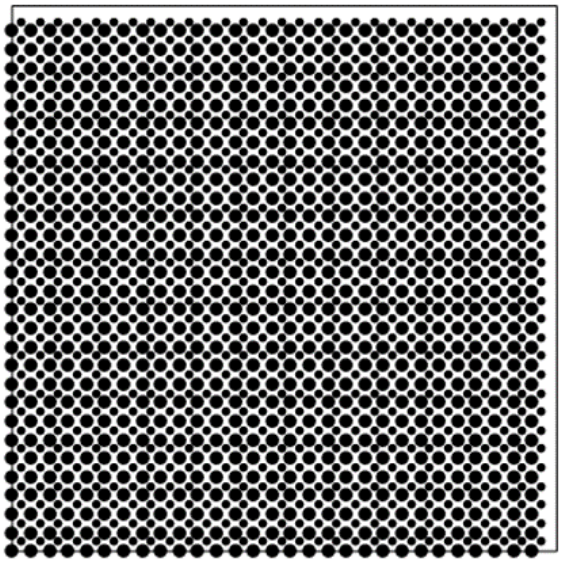

Figure 5: A crystal phase starting configuration. The big particles form squares, a small particle is placed at the center of each square, forming a centered square crystal. In this configuration, the number of big particles and the number of small particles are always equal.

If the starting configuration is a fluid phase, the number of big and small particles are calculated to match their respective packing fractions. This way the actual packing fraction is exactly the set value. The number of big and small particles can be set exactly if the packing fractions are chosen well. The way the particles are placed is very simple: A set of two random numbers is generated for every particle, representing its position. If the particle overlaps with any others, a new set of random numbers is generated. This is repeated untill all particles are placed. The result looks like figure 6.

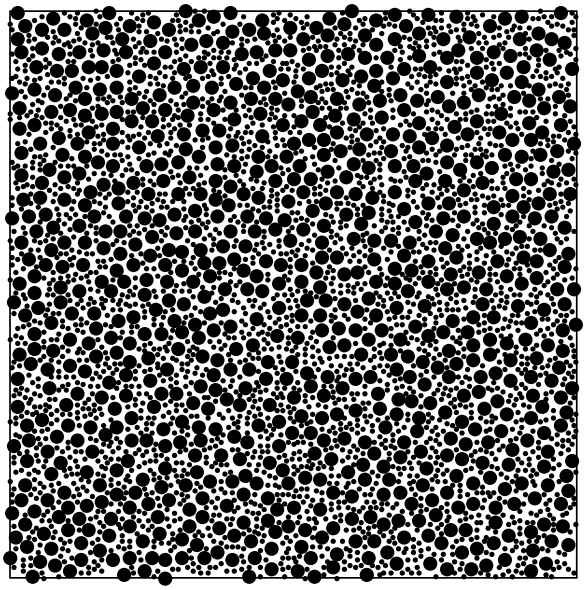

Figure 6: A fluid phase starting configuration. Particles are randomly placed in the box. Notice how here, there are many more small particles than big particles.

Now that all of the particles are in the system, it is divided into a grid of 1x1 squares. Then a record is made of which particles are in each grid square. Then the simulation starts moving particles. For each move, a random particle is selected and moved a random distance between Δ and $-\Delta$ in both the x- and y-directions. We use periodic boundary conditions, so if the particle moves outside the system, it is placed back into the system on the other side. Then the distance between the selected particle and each particle in the nine grid squares around it are calculated, as these are the only particles it could possibly overlap with. Only calculating these few distances significantly reduces the time it takes to run the simulation. We use the nearest image convention for calculating particle distances. What this means is that we assume there are identical copies of our system repeated endlessly in all directions. The particles in these copies are called the 'images' of the particles in the main system, and when a particle moves, all its images move the same way. This is also a way of explaining periodic boundary conditions: if a particle moves to a neighbouring copy of the system, one of its images moves into the system from another neighbour. The nearest image convention states that particles can only interact with the nearest image of another particle. This means that the largest distance between two particles in any direction is $L/2$. If the distance is larger than this, a different image must be closer, as the images are separated by distances of L. We implement this convention by subtracting/adding L for any distances greater/smaller than $\pm L/2$. For every distance calculated, the simulation checks for overlaps. If any overlaps occur, the selected particle is returned to its original position. Otherwise, its new position is recorded.

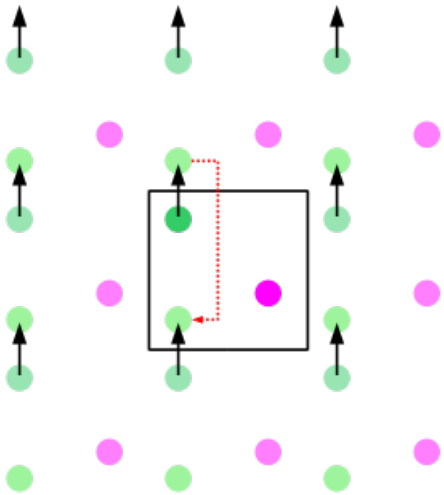

Figure 7: A visual aid for the nearest image convention and periodic boundary conditions. Each box represents a copy of the system. The green particle interacts with the image of the purple particle in the system to the left of its own, as this is the closest image.[Fei04] When the green particle moves out of its own system, one of its images moves back in on the other side.

These moves are repeated until the moment measurements are set to start. In our case, the pair correlation function g(r) is calculated. More specifically, the pair correlation function is separately calculated for big-big, small-small, and big-small pairs. We need all three of them for equations 5 through 17. To calculate the g(r) we start by realising that it should give the probability density of finding a particle at a distance r from another particle. This is approximated by making a histogram of the distances between every pair of particles, a separate histogram is made for each type of pair. The amount of measurement points for g(r) mentioned earlier is now used to calculate the size (dr) of each bin in the histogram. Each bin k holds the amount of particle pairs with distance between kdr and $(k+1)dr$, these amounts are called $Nbin_{bb}(r)$, $Nbin_{ss}(r)$, and $Nbin_{bs}(r)$. We only need to apply some normalisation factors to approximate g(r) using these.

$$g_{ij}(r) = \frac{Nbin_{ij}(r)}{Nid(r) \times (N_i \times N_j/N^2) \times N} \tag{18}$$

Where Nid is $Nbin$ if the system were a monatomic ideal gas. N is the total number of particles, and N_i is the number of particles of type i. The factor $(N_i \times N_j/N^2)$ is there to compensate for the fact that we are not counting all of the pairs in the system, just the ij-pairs. The calculation is repeated at specified intervals of moves, and g(r) is averaged over all the calculations at the end of the simulation.
After the g(r)s have been calculated, they can be used for the pole analysis described earlier.

3 Results

To find the structural crossover in our system, we ran 51 simulations with diferent relative packing fractions. The total packing fraction was kept constant at 0.5 and the small packing fraction was varied from 0.0 to 0.5. We should see crossover happening here as we have a simulation with only big particles on one end, and a simulation with only small particles on the other. The g(r)s we get from these simulations should exhibit wavelengts of roughly the size of the big particles and roughly the size of the small particles respectively. This means that somewhere in all the different packing fractions the wavelength has to change from one value to the other.

Unfortunately, we failed to get the code that was designed to perform the pole analysis outlined in section 2.3 to work. It failed to solve the set of equations because it simply took too long. Due to time constraints it was therefore necessary to measure the wavelengths by hand. This was done by measuring the distance between the three most prominent peaks in the graph and averaging the wavelength that way (see figure 8). It would have been better to use more peaks at higher r, but those are too small to be measured by hand. Because the distances are calculated by hand, they can only be considered accurate within a margin of ± 0.1.
The measured wavelength is plotted against the small packing fraction in figure 9.

The points marked in blue have a dominant wavelength close to the diameter of the big particles, and the points marked in red have a dominant wavelength close to the diameter of the small particles. The points marked in purple are ones where there are two possible wavelengths, this is why there are two purple points for each value of η_s. The wavelength has two potential values due to the appearance of a small peak at intermediate r that grows larger with increasing η_s (see figure 10). We were not certain of when we should start to consider this extra peak when calculating the wavelength. The points where this peak is visible, but still smaller than the one to its right are the ones marked in purple. Before $\eta_s = 0.13$ the peak is not visible and definitely does not contribute to the wavelength. After $\eta_s = 0.20$ the peak is larger than the next one, and thus definitely does contribute to the wavelength. Because the wavelength changes sharply across that interval, the cross over point is somewhere inside it.
We also ran simulations at total packing fractions of 0.4 and 0.6. The results of these simulations are plotted in figures 11 and 12. Once again, blue points have wavelengths of roughly σ_b, red points have wavelengths of roughly σ_s, and purple points could have either. We can combine these three sets of data to extrapolate a "cross-over area" in the (η_s, η_b)-phase space. This is done in section 4

We will first see if a quasicrystal has formed anywhere in the intervals we measured. To do that we make snapshots at different times of all the simulations. This way, if a quasicrystal forms, we can see it.
In this set of configurations, we did not find any quasicrystaline structures. This either means the total packing fraction is too low, or this is not the way to find a quasicrystal in a binary hard-sphere system.

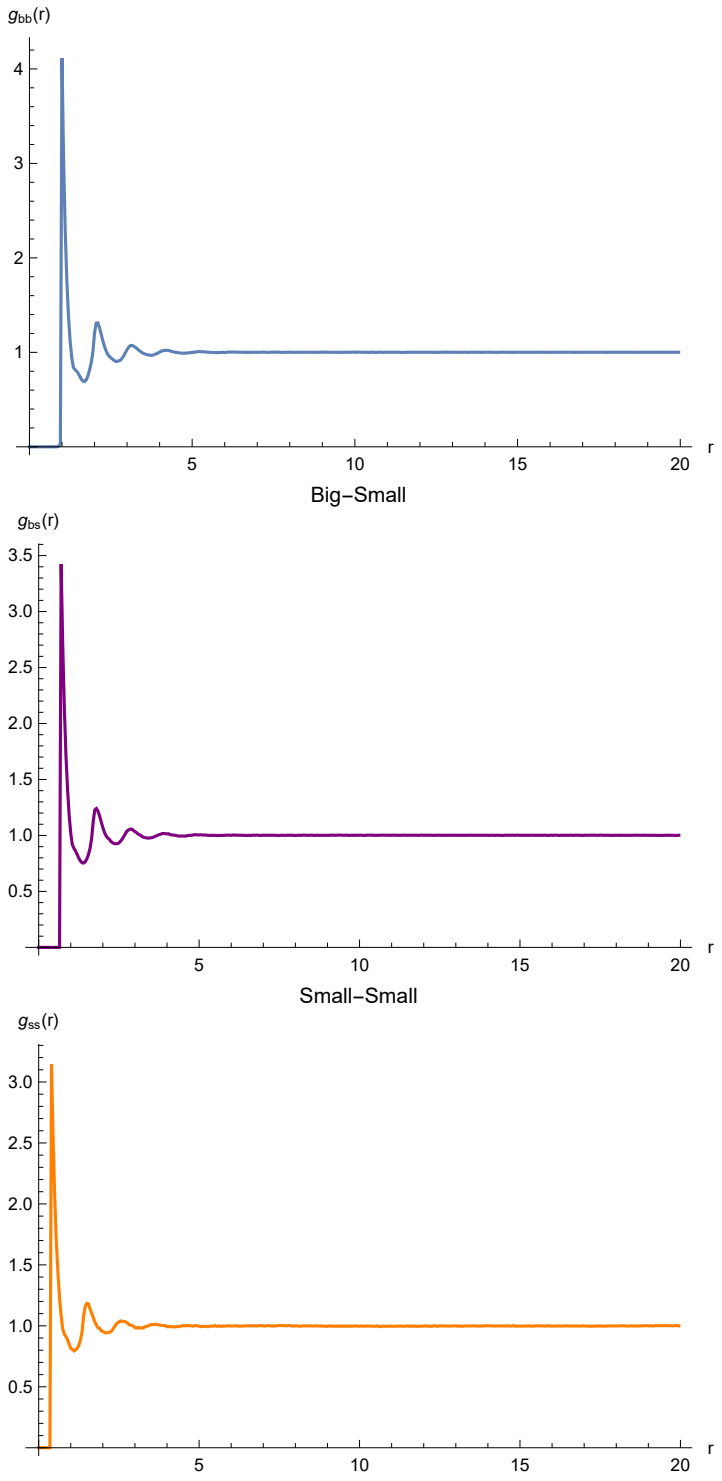

Figure 8: Some examples of $g_{bb}(r)$ (blue), $g_{bs}(r)$ (purple), and $g_{ss}(r)$ (orange). The wavelength is determined by measuring the r-coordinate of the first three peaks and averaging their distances. Optimally, we would use some later peaks, but those are too small to see. Distances are expressed in units of the big particle diameter.

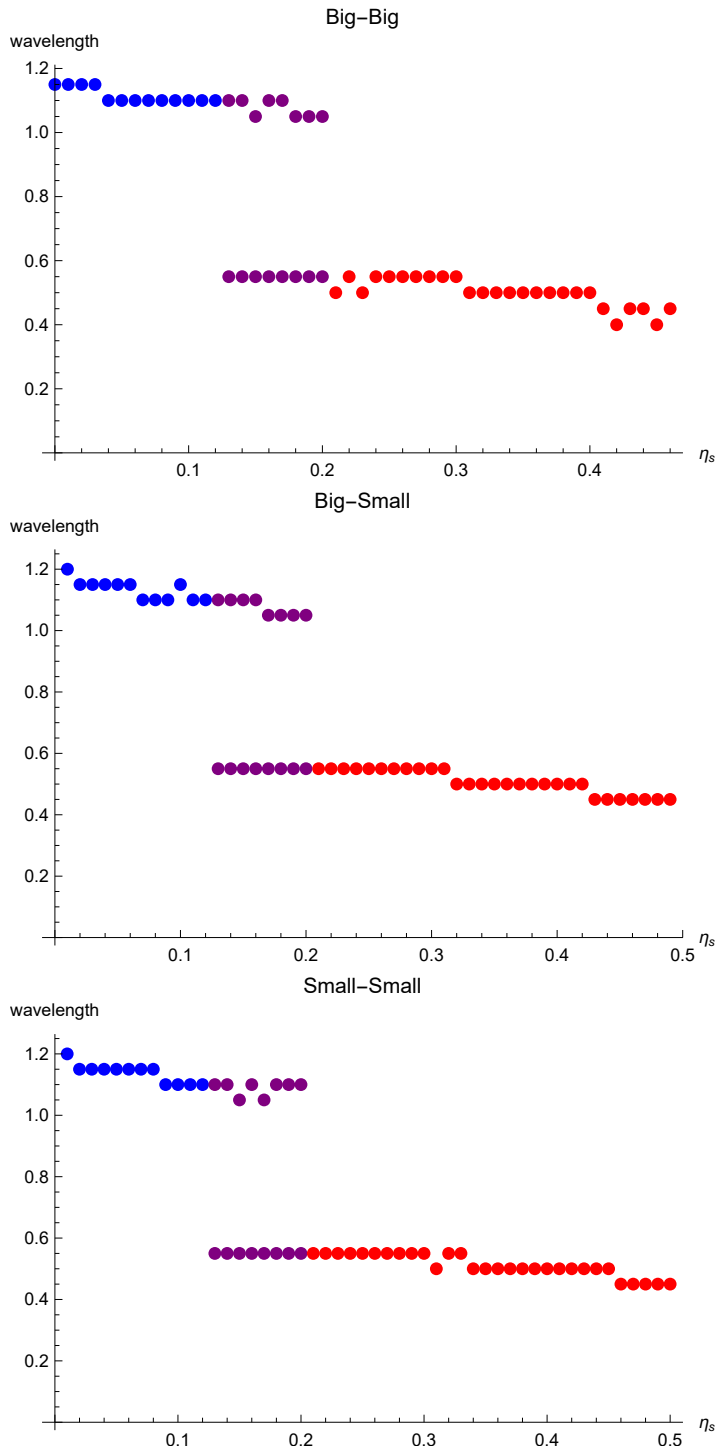

Figure 9: The dominant wavelength of $g_{bb}(r)$ (top), $g_{bs}(r)$ (middle), and $g_{ss}(r)$ (bottom) as a function of the small packing fraction (η_s). The total packing fraction (η) is 0.5. The big packing fraction (η_b) is given by $\eta_b = \eta - \eta_s$. the blue points clearly exhibit large wavelengths, the red points clearly exhibit short wavelengths, and the purple points could exhibit either. Aside from a few points, the three have a similar wavelength, as predicted by the theory.

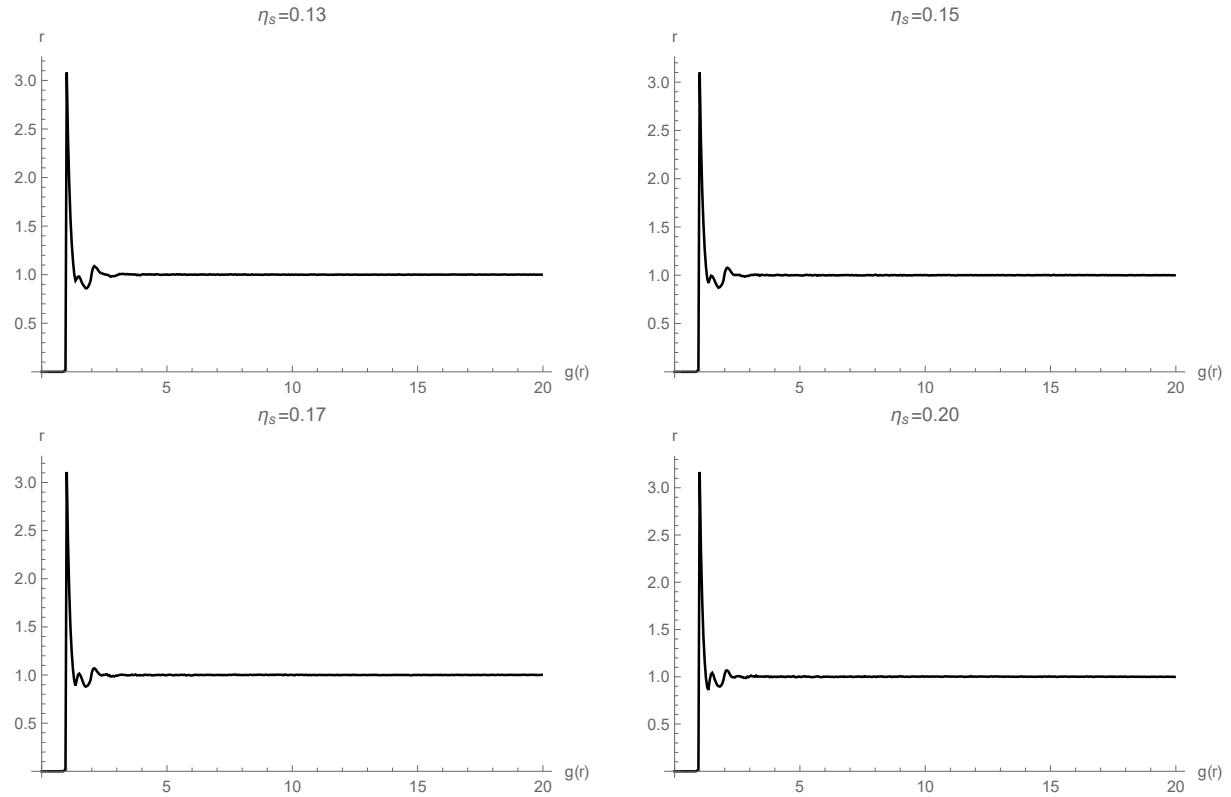

Figure 10: Some examples of $g_{bb}(r)$ for packing fractions in the purple region. At the bottom of the first peak, there is a small peak that grows larger with increasing η_s.

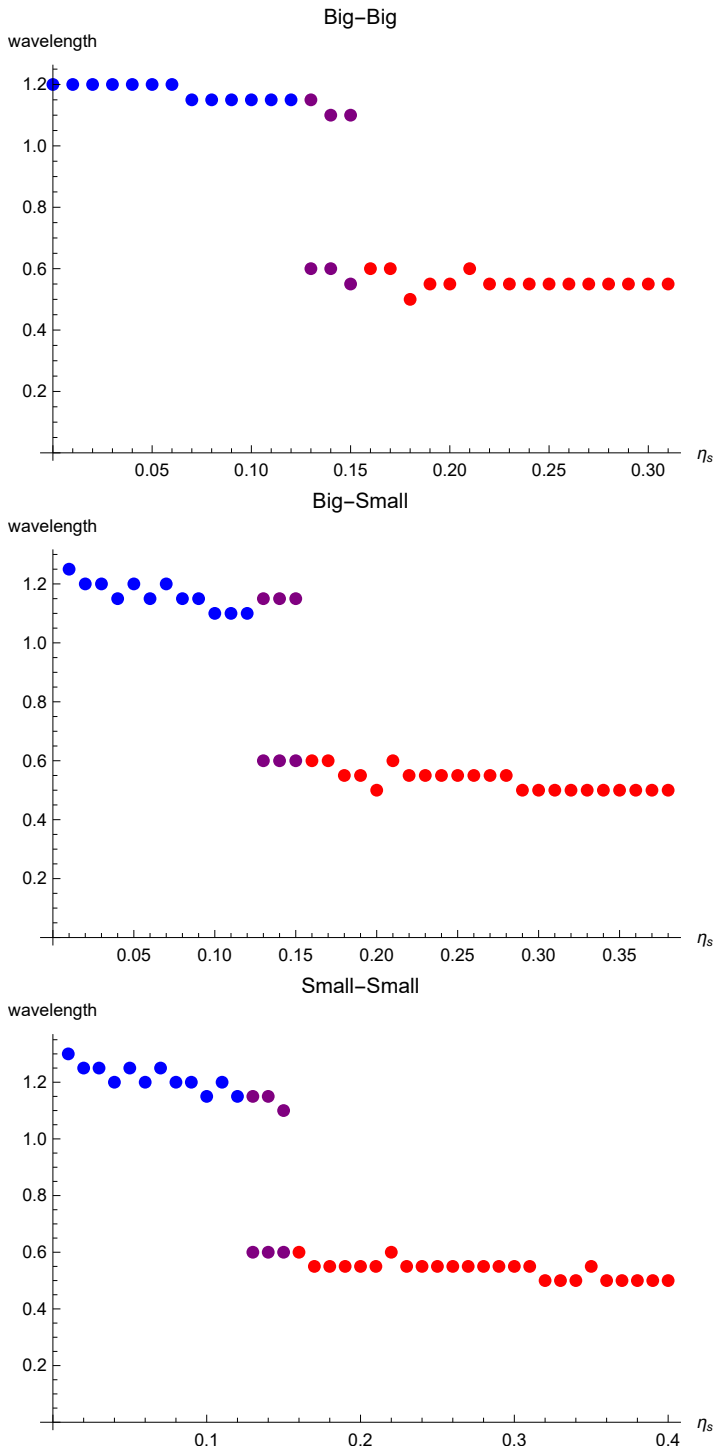

Figure 11: The dominant wavelength of g(r) for Big-Big, Big-Small, and Small-Small pairs as a function of the small packing fraction (η_s). This time, the total packing fraction (η) is 0.4. The big packing fraction (η_b) is given by $\eta_b = \eta - \eta_s$. the blue points clearly exhibit large wavelengths, the red points clearly exhibit short wavelengths, and the purple points could exhibit either. Aside from a few points, the three have a similar wavelength, as predicted by the theory.

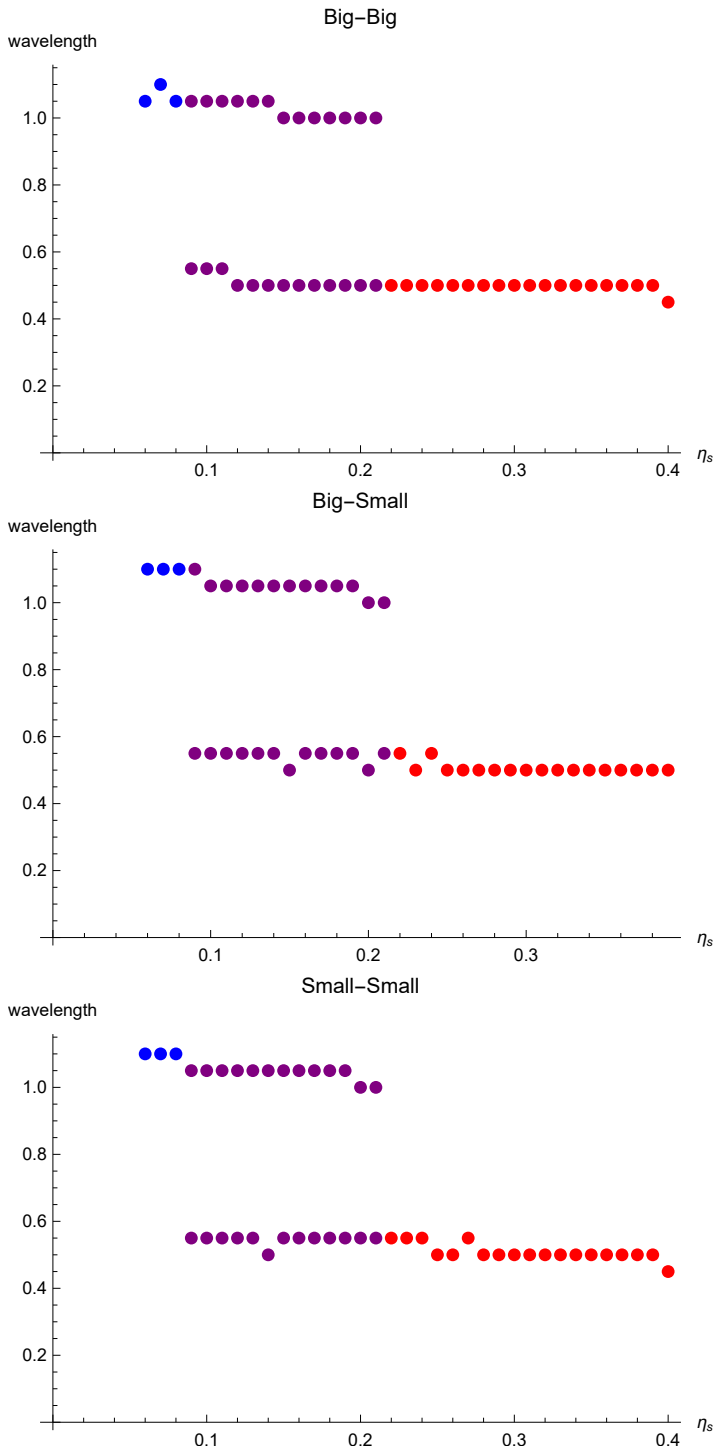

Figure 12: The dominant wavelength of g(r) for Big-Big, Big-Small, and Small-Small pairs as a function of the small packing fraction (η_s). This time, the total packing fraction (η) is 0.6. The big packing fraction (η_b) is given by $\eta_b = \eta - \eta_s$. the blue points clearly exhibit large wavelengths, the red points clearly exhibit short wavelengths, and the purple points could exhibit either. Aside from a few points, the three have a similar wavelength, as predicted by the theory. The points with eta_s below 0.6 and above 0.4 are missing because the simulations for these points failed to finish in time.

4 Conclusion & Discussion

Now that we have data from our simulations, we can extrapolate an area in (η_s, η_b)-space where structural crossover occurs (see figure 13). Combining this with a phase diagram, we could find an area in the space where structural crossover occurs and a solid state can form. Having both of these at the same time could result in a quasicrystal.

To extrapolate the cross-over intervals we obtained, we plot all our data in a (η_s, η_b)-space diagram, and connect the beginnings and the ends of all of the intervals we found with half-lines. Then the area in between those lines is where we expect crossover to occur.

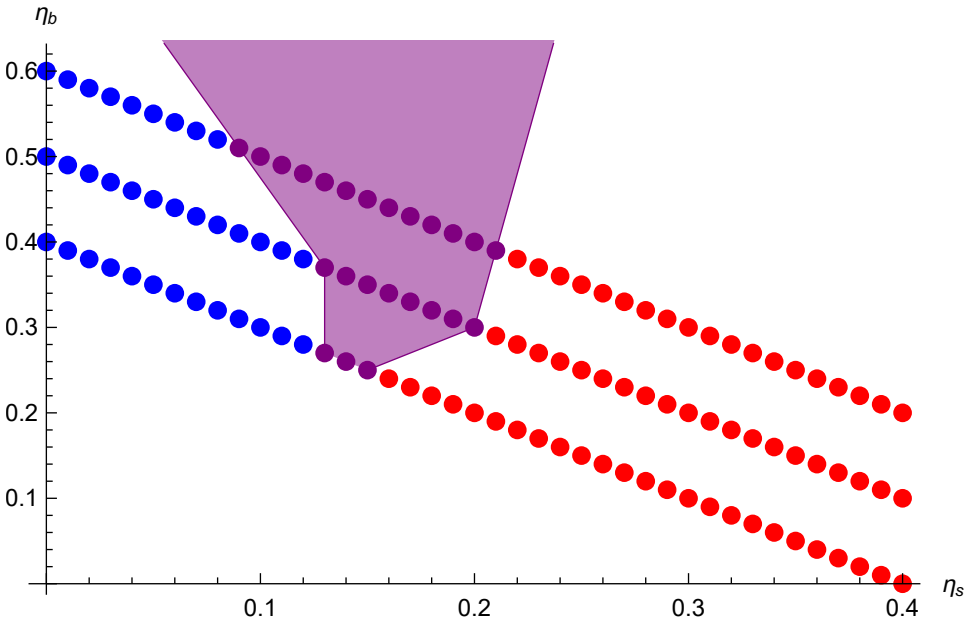

Figure 13: The data from figures 9 and 11 plotted in (η_s, η_b)-space. The purple points make up the cross-over intervals. The purple area shows where the structural cross-over may occur at higher packing fractions.

Now we have an area in which structural cross-over may occur. If we could combine this with a phase diagram made for a binary hard sphere mixture with size ratio $\lambda = 0.4$, we could find an overlap between the crystal phase and the cross-over area. If a quasicrystal can be found in this kind of system, This overlap area is a good place to investigate.

One problem with the result we have now is that while the theoretical cross-over line calculated by Statt et al.[Sta+04] curved downward like this area, it was much less steep. To confirm wether this is acutally a problem, more simulations would need to be ran at both higher and lower packing fractions. This way we could get a more complete picture of the cross-over area.

Unfortunately, we were not able to find a quasicrystal yet, as running more simulations at higher packing fractions would take too long to finish in time. However, the cross-over area we found should still help in finding binary mixture quasicrystals in the future.

4.1 Outlook

As mentioned earlier, to actually find a quasicrystal, a few more things need to be done.
More simulations need to be ran at different packing fractions to get a more clear picture of the structural cross-over line. Higher packing fractions need to be prioritised as they take more time to run, and it is more likely that a quasicrystaline phase can be found there. Having more data to extrapolate from will narrow the search area, making it easier to find a quasicrystal in the future.
Research into phase transitions in the (η_s, η_b)-space could allow for the creation of a phase diagram. This could then be combined with the data on the structural cross-over line to give an even better idea of where to search for quasicrystals.

References

[BB10] Stephen J. Blundell and Katherine M. Blundell. *Concepts in Thermal Physics*. 2nd ed. Vol. 1. Section 4.6. New York: Oxford University press, 2010. ISBN: 978-0-19-956209-1.

[DSh+84] D.Shechtman et al. "Metallic Phase with Long-Range Orientational Order and No Translational Symmetry". In: *Physical Review Letters* 53.20 (Nov. 1984), pp. 1951–1954.

[DKP94] Jean-Marie Dubois, Song Seng Kang, and Alain Perrot. "Towards applications of quasicrystals". In: *Materials Science and Engineering* (1994), pp. 122–126.

[Fei04] Adrian E. Feiguin, ed. *Boundary conditions*. accessed at: https://web.northeastern.edu/afeiguin/p4840/p131spring June 2004.

[FG57] F.Pearson and G.Rushbrooke. "XX.-On the Theory of Binary Fluid Mixtures". In: *Proceedings of the Royal Society of Edinburgh.Section A. Mathematical and Physical Sciences* 64.3 (1957), pp. 305–317.

[GS16] Branko Grunbaum and G. C. Shepard. *Tilings and patterns*. 2nd ed. Vol. 1. Dover Books on Mathematics. section 10.3. Dover Publications, June 2016. ISBN: 978-0-7167-1193-3.

[Kit96] Charles Kittel. *Introduction to solid state Physics*. 7th ed. Vol. 1. Chapter 1. John Wiley Sons, 1996. ISBN: 978-0-471-11181-8.

[LS84] Dov Levine and Paul Joseph Steinhardt. "Quasicrystals: A New Class of Ordered Structures". In: *Physical Review Letters* 53.26 (Dec. 1984), pp. 2477–2480.

[PJ17] Priyo Shankar Pal and Arun Jayannavar. "Interacting Multi-particle Classical Szilard Engine". In: (Jan. 2017).

[REv+94] R.Evans et al. "Asymptotic decay of correlations in liquids and their mixtures". In: *The Journal of Chemical Physics* 100.1 (Jan. 1994), pp. 591–603.

[RPe79] R.Penrose. "A Class of Non-Periodic Tilings of the Plane". In: *The Mathematical Intelligencer* 2.1 (Mar. 1979), pp. 32–37.

[Sta+04] Antonia Statt et al. "Direct observation in 3d of structural crossover in binary hard sphere mixtures". In: *The Journal of Chemical Physics* 144 (Apr. 2004), pages.

[Tal+09] Dmitri V. Talapin et al. "Quasicrystalline order in self-assembled binary nanoparticle superlattices". In: *Nature* 461 (Oct. 2009), pp. 964–967.